THE DORSA ARGENTEA FORMATION AND THE NOACHIAN-HESPERIAN TRANSITION: CLIMATE AND GLACIAL FLOW MODELING. K. E. Scanlon,[1] J. W. Head,[1] J. L. Fastook,[2] and R. D. Wordsworth,[3] [1]Department of Earth, Environmental and Planetary Science, Brown University, Providence, RI, USA. [2]School of Computing & Information Science, University of Maine, Orono, ME, USA. [3]School of Engineering and Applied Sciences, Harvard University, Cambridge, MA, USA. <*kathleen_scanlon@brown.edu*>

Introduction: The Dorsa Argentea Formation (DAF), a set of geomorphologic units (Fig. 1) covering ~1.5 million square kilometers near the south pole of Mars [1-3], has been interpreted as the remnants of a large south polar ice sheet that formed near the Noachian-Hesperian boundary and receded in the early Hesperian [4,5]. Determining the extent and thermal regime of the DAF ice sheet, as well as the mechanism and timing of its recession, can therefore provide insight into the ancient martian climate and the timing of the transition from a comparatively thick CO_2 atmosphere to the present climate. We used early Mars GCM and glacial flow model simulations to constrain climates allowing (1) development of a south polar ice sheet of DAF-like size and shape, (2) basal melting of this ice sheet in amounts and locations consistent with observed glaciofluvial landforms, and (3) recession of this ice sheet consistent with the preservation and crater exposure ages of landforms in the DAF.

Climate modeling: *Growth.* To determine climate conditions that favor the growth of a DAF-like ice sheet, we ran the LMD GCM with a 64x48 horizontal grid and 25 vertical levels; a pure CO_2 atmosphere; 0.75 the present solar flux [6]; and modern topography. Simulations were conducted with atmospheric pressure (P_{atm}) of 600, 1000, and 1500 mb; the martian atmosphere is unstable to CO_2 condensation at the poles at P_{atm} substantially higher than on modern Mars but lower than 600 mb [7; see 8 for similar findings with another Mars GCM]. Since a real gas that could warm early Mars sufficiently has not yet been identified, for "warm, wet" simulations, we added a grey gas, i.e. an artificial wavelength-independent absorption coefficient $\kappa = 2.5\times10^{-5}$, 5×10^{-5}, 1×10^{-4}, or 2×10^{-4} m^2 kg^{-1} [see 7].

Annual average surface temperature is nearly symmetric about the south pole on modern Mars [e.g. 9], reflecting the importance of surface radiation balance on planets with thin atmospheres [e.g. 10]. In early Mars simulations, with weaker insolation and a thicker atmosphere, annual average surface temperature has a wavenumber-3 pattern about the south pole. Correlation between altitude and annual average temperature increases with P_{atm} (at 41.8° obliquity, $r^2 = 0.37$ for 600 mb, 0.95 for 1500 mb), indicating that the south polar temperature pattern reflects both latitude-dependent insolation (important at low P_{atm}) and colder temperatures at higher altitude (important at high P_{atm} [11, 12]). The large 0°W and 90°W lobes of the DAF suggest that the DAF ice sheet formed in a climate where elevation significantly affected surface temperature. The ice distribution at the south pole is similar to the coldest part of the temperature pattern.

Surface melting is not significant in GCM simulations warmed only by CO_2. At relatively low P_{atm} (600 mb) and very high obliquity (60° or 70°), the DAF ice sheet undergoes some surface melting, but only for a few days each year. In all other pure CO_2 simulations, surface temperatures in the region never exceed 273°K.

Ablation. Ablation of the DAF ice sheet may have been caused by loss of the thicker early martian atmosphere, causing the south pole to become a less favored site for ice deposition; high-obliquity excursions, making ice less stable at the poles; or climate warming, leading to ice meltback. To investigate these possibilities, we initialized the GCM with ice as a uniform layer present only within the footprint of the present-day DAF, and setting a low P_{atm} (50 or 200 mb), increasing obliquity to the maximum value Mars is likely to have experienced even briefly (60° or 70°; [13]), or adding a grey gas.

At 60° and 70° spin-axis obliquity in a 1000 mb atmosphere, ice is removed from the DAF-like ice sheet at a rate of a few cm yr^{-1}. At 600 mb, removal rates are similar at 60° obliquity, but increase substantially at 70° obliquity, reflecting the greater importance of insolation in a thinner atmosphere. At 200 mb, the DAF-like ice sheet sublimes at a rate of a few tenths of mm yr^{-1}. At 50 mb, ice accumulates on the DAF-like ice sheet; while the altitude effect is unimportant at this pressure, the high albedo of the ice makes it an efficient cold trap in the insolation-dominated climate.

The regions of the DAF-like ice sheet that are removed first in "warm, wet early Mars" simulations (Fig. 2, between purple and red contours) are where eskers have been exposed longest according to crater counts [14]. The next longest-exposed esker population lies in a region of the ice sheet that is removed next (Fig. 2, between red and orange contours).

Glacial modeling: Since it does not simulate ice flow or basal ice temperature, the GCM alone cannot determine whether the extent of the south polar ice sheet in a given climate matches that of the DAF, or the amount and locations of basal melting. We used the University of Maine Ice Sheet Model (UMISM), adapted for Mars [5, 15, 16], to address these questions. We varied: (1) Atmosphere: 600 or 1000 mb CO_2, or 1000 mb CO_2 plus a grey gas; (2) global ice inventory: 2×10^7 – 2×10^8 km^3; (3) geothermal heat flux: 45 – 65 mW m^{-2} [17, 18].

In UMISM simulations with climate fields from pure CO_2 atmospheres, and those with weak grey gases ($\kappa < 1\times10^{-4}$), the extent of the south polar ice sheet is smaller than that of the DAF for all ice inventories and geothermal heat fluxes studied. Due to ice flow, the 0° lobe is

more prominent in the UMISM results than in GCM results with 1000 mb of CO_2, but the extent and thickness of the ice sheet do not match the extent of the DAF and the thickness inferred from the heights of the Sisyphi Montes. Instead, ice in these simulations preferentially accumulates on Tharsis and the rims of the Hellas and Argyre basins, with ice flowing west into Hellas and northwest into Argyre. In simulations with grey gas $\kappa = 2\times10^{-4}$, ice accumulates mostly on Tharsis. In simulations with grey gas $\kappa = 1\times10^{-4}$, ice accumulation is strongly favored at the south pole, and the south polar ice sheet resembles the DAF in shape and extent. The modeled ice sheet is somewhat larger than the DAF for global ice inventories $\geq 2\times10^{7}$ km^3, but with 10^{7} km^3, its extent closely matches that of the DAF (Fig. 3).

Conclusions: In GCM simulations with a thick (i.e. ≥ 600 mb) pure CO_2 atmosphere, an extensive ice sheet forms near the south pole, with lobes near 0°W and 90°W. The asymmetry of the DAF therefore likely reflects emplacement by an asymmetric ice sheet, rather than asymmetric erosion. In UMISM simulations, basal melting does not occur in the pure CO_2 atmospheres studied, regardless of the geothermal heat flux. The extent of the ice sheet in the pure CO_2 simulations is smaller than that of the DAF regardless of ice inventory, but in artificially warmed simulations, the ice sheet is larger than the DAF unless global ice inventory is $< 2\times10^{7}$ km^3 ($\lesssim$ 137 m GEL). We therefore conclude that the DAF ice sheet reached its maximum extent in a climate between our "cold and icy" and "warm and wet" endmembers, in a climate similar to our warm simulations with a small ice inventory, or in a cold climate that experienced periodic warming. Eskers in the DAF are located in the regions where ice first ablates from a DAF-like ice sheet in GCM simulations, and where basal melt fluxes are highest in "warm, wet" UMISM simulations; no eskers are observed where basal temperatures are warmest in the "cold and icy" climate endmember simulations, and few occur in association with glaciovolcanic features. We therefore conclude that the eskers in the DAF formed from a combination of surface melting and "top-down basal melting" [5] during warm intervals. Crater ages for the eskers [14] are consistent with this hypothesis and the hypothesis that they formed in the same era as the equatorial valley networks.

References: [1] Tanaka, K.L., and D.H. Scott (1987), *USGS Map I–1802-C.* [2] Tanaka, K.L., and E.J. Kolb (2001), *Icarus, 154*, 3–21. [3] Tanaka, K. L. et al. (2014), *PSS, 95, 11–24*; [4] Head, J. W., and S. F. Pratt (2001), *JGR, 106,* 12275-12299; [5] Fastook, J.L., et al. (2012), *Icarus, 219,* 25-40. [6] Gough, D. O. (1981), *Physics of Solar Variations*, 21–34, Springer Netherlands; [7] Wordsworth, R. D., et al. (2015), *JGR: Planets, 120,* 1201–1219; [8] Soto, A., et al. (2015), *Icarus, 250,* 553-569; [9] Kieffer, H. H. (2013), *JGR: Planets*, *118*, 451-470. [10] Read, P. L., and S. R. Lewis (2004), *The martian climate revisited,* Springer Science & Business Media.; [11] Forget, F., et al. (2013), *Icarus, 222,* 81-99; [12] Wordsworth, R., et al. (2013), *Icarus, 222,* 1-19; [13] Laskar, J., et al. (2004), *Icarus*, *170*(2), 343-364. [14] Kress, A. M., and J. W. Head (2015), *PSS, 109,* 1-20; [15] Fastook, J. L., et al. (2008), Icarus, 198, 305-317; [16] Fastook, J. L., and J. W. Head III (2015), *PSS, 106,* 82-98; [17] Montési, L. G. J., and M. T. Zuber (2003), *JGR: Planets, 108,* E6; [18] Solomon, S.C. et al. (2005), *Science, 307,* 1214–1220.

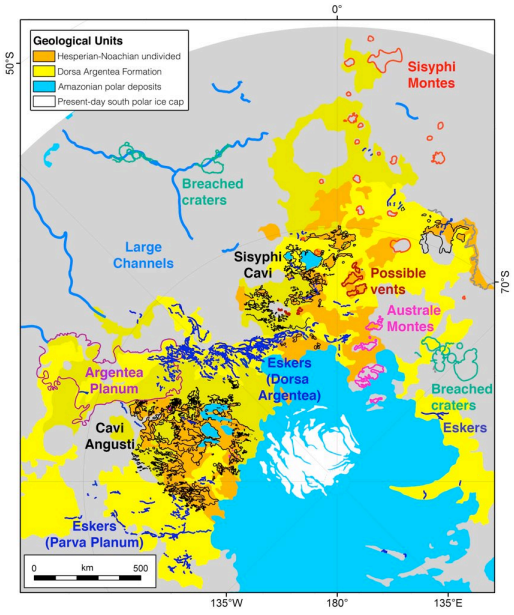

Fig. 1. The DAF: units as mapped by [1], with glaciofluvial and glaciovolcanic features outlined and labeled.

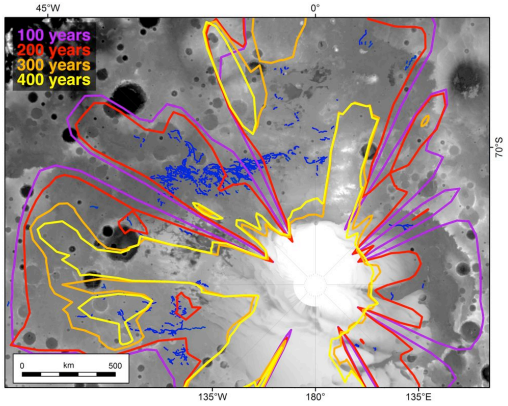

Fig. 2. Location of the ~20 m GCM ice contour after 100 – 400 years of ice evolution (colored contours) on shaded MOLA topography. Eskers are mapped as dark blue lines.

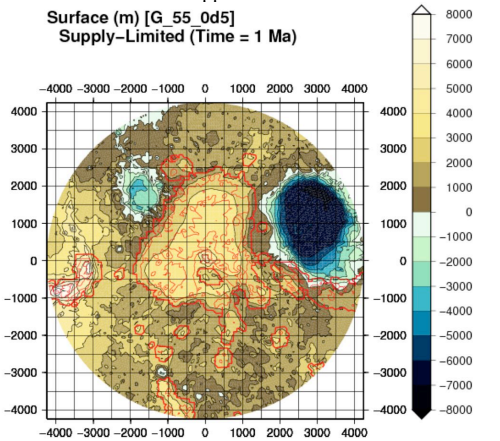

Fig. 3. UMISM south pole-centered ice surface in the grey $\kappa = 1\times10^{-4}$ scenario. Ice thickness shown as red contours at intervals of 500 m.